Optimization of interfacial adhesion and mechanical performance of flax fiber-based eco-composites through fiber fluorination treatment

Olivier Téraube, Jean-Charles Agopian, Monica Francesca Pucci, Pierre-Jacques Liotier, Pierre Conchon, Éric Badel, Samar Hajjar-Garreau, Honorine Leleu, Jean-Baptiste Baylac, Nicolas Batisse, et al.

Optimization of interfacial adhesion and mechanical performance of flax fiber-based eco-composites through fiber fluorination treatment

Olivier Téraube [a,b,*], Jean-Charles Agopian [a,b], Monica Francesca Pucci [c], Pierre-Jacques Liotier [d], Pierre Conchon [e], Éric Badel [e], Samar Hajjar-Garreau [f], Honorine Leleu [b], Jean-Baptiste Baylac [b], Nicolas Batisse [a], Karine Charlet [b], Marc Dubois [a]

[a] Université Clermont Auvergne, Clermont Auvergne INP, ICCF, BP 10448, 63000, Clermont-Ferrand, France
[b] Université Clermont Auvergne, Clermont Auvergne INP, Institut Pascal, BP 10448, 63000, Clermont-Ferrand, France
[c] LMGC, IMT Mines Alès, Univ Montpellier, CNRS, Alès, France
[d] Polymers Composites and Hybrids (PCH), IMT Mines Alès, Alès, France
[e] Université Clermont Auvergne, INRAE, PIAF, 63000, Clermont-Ferrand, France
[f] Institut de Science des Matériaux de Mulhouse, CNRS-UMR 7361, Université de Haute-Alsace, 68057, Mulhouse, France

A B S T R A C T

Natural fibers, such as flax, are more and more used as biobased reinforcement for eco-composites manufacturing but their natural polarity makes them incompatible with most polymers (mostly dispersive). Nowadays, treat-ments such as torrefaction are known to reduce the polarity of natural fibers and thus increase the mechanical performance of the reinforced composites. However, these treatments could harm fibers and limit the gain in performance. Thereby, the use of a controlled fluorination treatment allowed, *via* the grafting of fluorine on the fiber surface, to decrease the polarity of these fibers while maintaining an equivalent Young's modulus and limiting the reduction of at break performance to just ~30 %. Therefore, by incorporating these fluorinated reinforcements in an epoxy matrix and by mechanically testing these composites, not only superior mechanical performances to those reinforced by raw fibers, but also superior to torrefied fiber-reinforced composites were measured, *e.g.*: the flexural modulus increased by 25 % after fluorination *vs.* 10 % after torrefaction and the flexural strain at break was enhanced by 10 % after fluorination *vs.* decrease by 35 % after torrefaction).

Keywords:
Natural fibers
Porosity
Wettability
Surface treatment

1. Introduction

In most industries, the objective is to obtain materials of better or at least equivalent properties, while reducing their weight, cost and carbon footprint. In this context, vegetal fibers used as polymer matrix reinforcements to manufacture "eco-composites", are prime candidates to solve the above-mentioned issues [1].

Among natural fibers, and especially for high value-added applications, flax fibers are often considered as one of the best bio-based reinforcements for composites [2]. Indeed, their high specific mechanical properties, comparable to glass fiber ones, and even, to a part of aramid fibers [3,4], their density, lower than carbon fibers and their low cost next to other reinforcement fibers (less than 2 $/Kg vs. 2–3.5 $/Kg for E-glass and 8–11 $/Kg for carbon fibers [4]) make them a serious challenger to synthetic fibers, as part of pure natural fibers composites, but also when employed as hybrid (coupling of natural fibers and synthetic fibers in order to combined different combining the strengths of each reinforcement) [5,6].

When dealing with composite materials, one of the key points is to ensure the physico-chemical compatibility of fibers with the polymer matrix to obtain an optimal mechanical performance. Indeed, a weak reinforcement/matrix compatibility will lead to a poor reinforcement wetting by the polymer and to the appearance of microvoids at the reinforcement/matrix interface. Cavities are established as mechanical weakness points, from which cracks can emerge and propagate under stress [7–10].

Regarding this issue, flax fibers, and more widely lignocellulosic reinforcements, are disadvantaged. Indeed, the strong concentration of hydroxyl and carboxyl groups in their chemical structure, results in a high polarity γ_s^p of ≈26.0 mN/m whereas a dispersive component γ_s^d of ≈34 mN/m is typically measured [11]. They are thus inherently incompatible with mostly dispersive polymers, and therefore difficult to

* Corresponding author. Université Clermont Auvergne, Clermont Auvergne INP, ICCF, BP 10448, 63000, Clermont-Ferrand, France.
E-mail address: olivier.teraube@outlook.com (O. Téraube).

wet by these latter during composite processing [12–14]. This also makes them sensitive to water and moisture sorption. However, water absorption and desorption cause swelling and shrinkage, and this change in fiber morphology may lead to cracks in the composite structure [1,9].

Numerous chemical and physical treatments were developed in order to counter the above-mentioned weaknesses of lignocellulosic reinforcements on the one hand, and fully exploit their potential on the other hand, by reducing the hydrophilicity of these fibers.

Among them acetylation can be mentioned first. This chemical treatment developed in 1928 that is an esterification reaction between the free –OH groups natural product and acetic anhydride in order to replace these hydroxyl groups an acetyl groups reducing hygroscopicity to less than 20 % moisture in a saturated environment (90 % relative humidity) [15,16]. Thanks to this treatment, the adhesion between a hydrophobic polymer matrix and acetylated fibers is increased (and consequently the mechanical properties of composites) [17,18]. However, high cost of this treatment, coupled with the limited supply of acetic anhydride and the latter's toxicity, limit the use of acetylation.

Alkaline treatment, or mercerization, is also known to reduce the polarity of fibers while increasing the mechanical properties of the fibers. This treatment is based on the reaction of fibers with sodium hydroxide (NaOH). Thanks to this treatment, compatibility with both matrices thermoplastic and thermoset resin is increase [17,19] with a gain up to 30 % in epoxy-flax fiber composites [19].

Still on chemical treatment, maleic anhydride is used to create covalent bonds between fibers and polymers, improves adhesion, but its toxicity (CMR) limits its use [20–24]. Ultrasonic silane treatment also demonstrates very interesting efficiency in order to enhance mechanical properties of composites with, for example a 15 % improvement in ultimate tensile strength, 20 % in hardness, 34 % in ultimate flexural strength, and 18 % in impact properties [25]. Finally, thermal treatment [15,16,26] or electric discharge [17,18] appear as physical way to reduce vegetal fibers' polarity. However, this kind of treatment generally come with a significant reduction in the mechanical performance of these fillers.

Overall, these treatments allowed to decrease the polarity of the lignocellulosic fibers and thus, improved the overall mechanical behavior of the manufactured composites, even if elementary fibers and yarns have been embrittled [19]. However, current industrial treatments used to compatibilize vegetal fibers with mostly dispersive polymers are costly, both time and energy consuming, and/or harmful to the environment and people by using toxic solvents or chemicals. New eco-friendly methods must be then developed to be in full accordance with the concept of "eco-composite". For this purpose, innovative "green" processes for achieving this compatibilization without impacting the environment must be investigated [27–35], keeping in mind the necessary scale-up to an industrial level, the additional investments and/or the development of new technologies.

Direct fluorination *i.e.* treatment of the substrate with pure elemental fluorine or fluorine diluted with an inert gas (nitrogen, helium etc.), is frequently used at an industrial scale in order to enhance various properties of polymeric materials [36]. In mild conditions, this chemical treatment acts only on a thin part of the substrate (layer with ~0.01–10 μm depth) without modifying the bulk, allowing the initial properties of raw materials to be maintained [36–39]. If various properties are brought with this fluorinated layer, such as a reduction of permeability to hydrocarbons and other compounds, an enhancement of friction properties, an improvement of chemical resistance [36,38,40], direct fluorination mainly allows to reduce the polar character of materials [37,38,41–44]. Moreover, as a gas/solid reaction, fluorination is performed without using toxic solvent, in a closed reactor without release of any toxic substance in the atmosphere, and can even be spontaneously achieved at room temperature; this treatment thus exhibits a low environmental footprint. Moreover, it is a quick reaction, without any human contact with the reactant, reproducible, which is thus presenting all advantages required for an eco-responsible industrial way to make vegetable fibers less polar (Life Cycle Assessment (LCA) of the treatment will have to be carried out to firmly conclude on its sustainability).

It has been previously proved [45] that a treatment under molecular fluorine (F_2) of flax fibers allows to covalently graft fluorine atoms on the outmost surface of lignocellulosic materials, in substitution of hydroxyl groups responsible for hydrophilicity. This grafting allowed to significantly decrease fiber polarity without modification of their bulk mechanical performance [45]. Then this treatment should allow to improve the wetting of fibers by hydrophobic polymers and consequently the quality of fiber –matrix interface. This should result in a significant decrease in the porosity of a composite reinforced with fluorinated flax fibers, in comparison with a composite reinforced with raw flax fibers. The composite reinforced by fluorinated flax fibers should then have higher mechanical performance, and a better health and durability during a wet-environment aging, without using any chemical coupling agent harmful to the environment.

The purpose of the present work is, firstly, to validate these statements by applying a fluorination treatment on flax fibers at a pilot scale, and secondly to manufacture eco-composites based on these flax fibers, either left as-received or fluorinated. Since these eco-composites (flax/epoxy) are manufactured in the exact same way *via* Vacuum Resin Infusion, their mechanical performance and their porosity rate can be compared.

In addition, fiber torrefaction treatment is also known to increase the overall mechanical behavior of composites reinforced by such fibers [19]. Therefore, this treatment is also applied to our flax fibers in order to manufacture composites and compare fluorination and torrefaction treatments.

2. Materials and methods

2.1. Materials

Flax reinforcements were pieces of FlaxTape™ 110, purchased from Eco-Technilin. These not-sized fibers are a 40 cm width tape of unidirectional flax fibers with an areal weight of 110 g/m^2. A part of these reinforcements were used "as received" (noted "raw" in the following) to manufacture composite materials, but others have also undergone torrefaction or fluorination treatments as described below.

Composites were manufactured by Vacuum Assisted Resin Transfer Molding (VARTM) and two different resins were use.

- A 100 % petroleum-based epoxy resin Resoltech 1050 coupled with 1056S hardener. Resin and hardener were mixed together with a 100/35 wt ratio. Its viscosity is 1300 MPa s at 23 °C.
- A bio-based epoxy resin SR Infugreen 810 from Sicomin, which is produced with around 38 % of carbon from plant origin and coupled with SD 8824 hardener. Both components were mixed with a 100/22 wt ratio. The viscosity of this resin is 290 MPa s at 20 °C.

Based on the tensiometric tests methods described in Ref. [46], polar and dispersive components of surface tension of uncured resin were measured in standard conditions, and results are displayed in Table 1. It has to be noted that the absolute error of γ_s^p of the Infugreen matrix goes below 0 mN/m, which is due to the calculation method of the relative error, as polar and dispersive components of surface tension cannot be negative.

Table 1
Measured surface tension and its components for the 1050 and Infugreen resins at 20 °C.

Matrix	γ_s^p (mN/m)	γ_s^d (mN/m)	$\gamma_s^{tot.}$ (mN/m)
1050	5.5 ± 2	26.4 ± 2	31.9 ± 2
Infugreen	0 ± 2	46.7 ± 2	46.7 ± 2

2.2. Fiber treatments

2.2.1. Fluorination

Fluorination of not-sized flax fibers was performed in a 50 L passivated nickel reactor (covered with NiF_2) under static conditions. The flax fibers were distributed over 4 trays (Fig. 1b) and introduced into the fluorination reactor. Each of these pieces is 65 cm long and 21 cm wide (Fig. 1a).

The reactive gas consists in a mixture of pure elemental fluorine, purchased from Solvay Fluor (less than 0.1 vol % of admixtures, mainly oxygen), and pure nitrogen (99,999 % purity). Before each reaction, fibers were first outgassed during 2h under primary vacuum (10^{-3} mbar) at 120 °C within the reactor. Then, the heating was turned off, and the reactor was left to cool down overnight.

After that, the reactor (still under vacuum, 10^{-3} bar) was filled. First, the pump was switched off and N_2 was injected in the reactor during 5 min at a 400 mL/min flow rate. Then, the reactive F_2/N_2 mixture was introduced during 20 min in the reactor with N_2 and F_2 flow rates which were respectively equal to 400 and 100 mL/min. When the absolute pressure inside the reactor was at −760 mbar (after 20 min, the ratio F_2/N_2 being then 1/5 vol/vol), F_2 flux was stopped and N_2 was added (600 mL/min) alone in the reactor until an absolute pressure of 1 bar was reached (F_2/N_2 = 2/34 vol/vol). Once the target of 1 bar was reached, the reactor was immediately flushed with pure nitrogen gas overnight to both stop the reaction and remove traces of unreacted F_2 and HF towards a soda lime trap (part downstream of the fluorination reactor, filled with soda lime, intended to scavenge the fluorinated species to avoid their release into the atmosphere). Finally, the fibers were once again outgassed for 1h under nitrogen at 120 °C to ensure a full removal of all fluorine-based gases from the sample surface. Those operating conditions were extrapolated from treatments in a smaller reactor of 5L [45], taking into account the specification of the gas flowmeter (maximal flows).

2.2.2. Torrefaction

Torrefaction of not sized flax fibers was carried out according to the optimized treatment described by Berthet et al. in order to improve fiber/matrix adhesion in a biocomposite [16]. The treatment was realized in the same reactor as the one used for fluorination, and in the same configuration (four 65 cm long trays), but time and set-up temperatures were adapted to the oven size. Thereby, once the fibers were placed in the reactor, the latter was put under vacuum (10^{-3} mbar) for 30 min, and then completely filled with N_2 (600 mL/min). Then, gas circuit was opened and a constant flow of N_2 (100 mL/min) was applied and the following sequence was performed.

- Step 1: Drying at 110 °C for 1 h.
- Step 2: Heating at 220 °C for 1.5 h.
- Cooling overnight.

At the end of this procedure, a color gradient was observable on all fiber tapes (Fig. 1c), due to the fact that the piece of the tissue located at 0 cm was exposed to a higher temperature than the piece positioned at 65 cm. Moreover, the length of the fiber brown piece (representative of the torrefaction treatment) is shorter on the reinforcements placed on tray 4 than the ones on tray 1, highlighting the oven spatial temperature gradient (see Fig. 1d). To counter this, trays were first rotated by 180° (the area previously located at 0 cm is now located at 65 cm and *vice versa*) as well as a change of position: fibers of tray 1 were exchanged with those of tray 4 and those of tray 2 were inverted with those of tray 3. After that, fibers underwent a second time the torrefaction sequence described above, and this time a color homogeneity was achieved (Fig. 1e), evidencing a homogeneous treatment on all fiber length.

2.3. Fibers characterization

Once both treatments previously described were performed, treatment homogeneity was evaluated because of the pilot scale of the reactor.

2.3.1. Chemical homogeneity of fluorination treatment

For fluorination treatment, chemical homogeneity was checked using 3 different chemical characterizations at different scales. FT-IR spectra were recorded in ATR mode (diamond crystal) using a Nicolet 6700 FT-IR spectrometer from Thermo Scientific in 32 scans with a resolution of 4 cm^{-1}. In addition, ^{19}F solid state NMR experiments were also carried out. To obtain the spectra, flax fibers were cut and incorporated into a 2.5 mm rotor for spinning at 30 kHz into a magic-angle spinning (MAS) probe. The acquisition sequence was constituted of a single 90° pulse length of 3.5 µs. ^{19}F chemical shifts were externally referenced to CF_3COOH and then referenced to $CFCl_3$ ($\delta_{CF_3COOH} = -76.6$ ppm vs δ_{CFCl_3}). Finally, X-ray photoelectron spectroscopy (XPS) measurement was carried out in order to investigate the surface composition of fibers. Experiments have been conducted on a VG Scienta-SES 2002 hemispherical analyzer, using a monochromatic Al K_α (1486.6 eV) X-ray source radiation and an electron gun for charge effect compensation. Spectra were fitted with Gaussian-Lorentzian component profiles after a Shirley background subtraction, thanks to the casaXPS software 2.3.18 Ltd., Teignmouth, UK [47], and all peaks were repositioned by positioning the Csp^3 (C–C/C–H) C1s line at 284.9 eV.

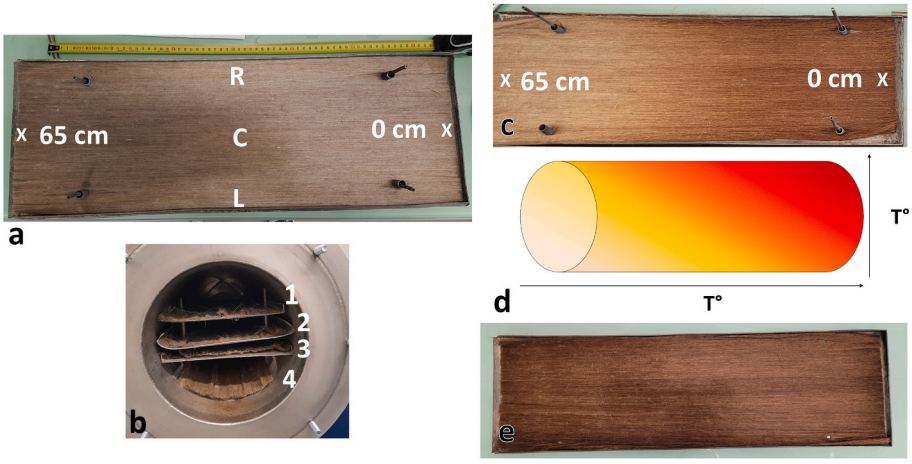

Fig. 1. a) Picture of one tray and b) the 50 L fluorination reactor with 4 trays inside. c) Torrefied fibers after the 1st torrefaction sequence, d) Schematic representation of the temperature gradient in the oven, e) Torrefied fibers after the 2nd torrefaction sequence.

2.3.2. Torrefaction treatment homogeneity

To check the homogeneity of torrefaction treatment, pictures of fibers were taken using a Fujifilm X–S10 camera equipped with a Fujinon XF18-55 mm F2.8–4 R LM OIS lens. A manual mode was performed at 55 mm, iso160, *f*4, 1/8s of exposure time, with the exact same light and the same white balance. Then, RAW files have been uploaded in Affinity photo software, white balance have been fixed to 4000K (color temperature of the room lighting) for all pictures in order to adjust white of the different pictures and these have been developed by the software. From this moment, pictures have not been modified in any way. Still using Affinity photo, color picker tool was used to identify the color of the selected pixel. For each sample, 25 picking were realized in the CIE L*(lightness), a* (X axis from green (−) to red (+)) and b* (Y axis from blue (−) to yellow (+)) colorimetric representation; this model is commonly used to study the color variations of different substrates [48–50], especially lignocellulosic ones [51,52].

2.3.3. Surface energy measurement

In order to estimate the change in the surface energy due to treatments, the contact angles between fibers and different liquids are necessary. Whereas the "sessile drop" technique is classically carried out [53], the cylinder shape of fibers increases the uncertainty and question the reproducibility of positioning liquid drops on fibers. Thereby, in order to determine the surface energy of the flax fibers, another method must be carried out. Indeed, amongst the different techniques [54–57], Wilhelmy method appears as the most convenient. First described by Qiu et al. [55], it is based on the use of a Wilhelmy balance and the Wilhelmy relationship (1)

$$F = \gamma_{liq}\, p \cos\theta \tag{1}$$

where F is the capillary force (mN), p (m) the wetted length, θ (°) the contact angle and γ_{liq} (mN/m) the surface tension of the liquid. The procedure which has been carried out is described in a previous work [58]. Measurements were performed using a Krüss K100SF tensiometer. A single fiber was immersed in n-hexane (Sigma-Aldrich, ReagentPlus 99 %) which is considered as totally wetting ($\theta \approx 0°$). From there, the Wilhelmy equation allowed the wetted length of the fibers to be determined. Then, knowing the wetted length and the tabulated γ_L, the contact angle was determined using equation (1) by measuring the force F exerted by the testing liquid on the fiber.

Thereby, two different liquids (water and diiodomethane from AlfaAesar, 99 %, stab. with copper) were considered; the Owens-Wendt equation (equation (2)) allowed the polar γ^p_{fibre} and the dispersive component γ^d_{fibre} of the surface energy of fibers to be identified [59].

$$\frac{\gamma_{liq}(1+cos(\theta))}{2\sqrt{\gamma^d_{lq}}} = \sqrt{\gamma^p_{fibre}}\left(\frac{\sqrt{\gamma^p_{liq}}}{\sqrt{\gamma^d_{liq}}}\right) + \sqrt{\gamma^d_{fibre}} \tag{2}$$

2.3.4. Flax fibers tensile tests

Finally, to evaluate the impact of the direct fluorination treatment on the mechanical properties of flax fibers, tensile tests were performed on fibers, in compliance with the NF T 25-501-2 standard on an Instron 5543 tensile testing machine equipped with a 50 N load cell and pneumatic grips.

Test were performed using the following procedure on (at least) 50 samples for each treatment.

- Single flax fiber was glued on a Kraft-paper frame with a central hole of 10 mm (gauge length);
- Average fiber diameter was obtained considering 3 measurements of the diameter under microscope at 1000× magnification;
- Kraft-paper frame with the fiber was placed into the pneumatic grips, then frame edges were cut and the test was started with a constant crosshead displacement rate of 1 mm/min.

2.4. Composite manufacturing

Composite plates were manufactured by Vacuum Assisted Resin Transfer Molding (VARTM). The fibers are a tape of unidirectional flax fibers with a real weight of 110 g/m^2. In each composite, 6 fibers plies of 400 mm long and 40 mm wide were introduced. Therefore, in each composite, 6 × 1.76 g of fibers were introduced, *i.e.* 10.56 g. To realize these plates, a two-part PMMA mold with a 400 mm long, 40 mm wide and 3 mm thick cavity was used. For each infusion, 6 fiber plies were cut (length in the fiber direction) at the mold cavity dimensions and stacked within it (Fig. 2a). Then, two cylindrical gaskets (in black on Fig. 2a) were placed in the location provided, to ensure the vacuum tightness of the mold. After that, the counter mold was placed, and the two parts of the mold firmly closed and held in position using C-clamps (Fig. 2b). Thereafter, resin was mixed with its corresponding hardener and mixture was stirred for 5 min. Once mixed, the resin pot was connected to the mold by a plastic pipe, and the whole infusion device was put under vacuum (10^{-3} bar), ensuring a full matrix degassing. After 5min, circuit upstream of the resin was returned to atmospheric pressure, while the mold was still under vacuum, driving the resin along the mold. Once the manufacturing was achieved, the set was left 24 h to obtain a composite plate cured enough to be demolded. Then the plate was demolded and dried for, at least, 2 weeks at room temperature.

For each reinforcement types (raw, torrefied and fluorinated) and resin (1050 and Infugreen), 4 plates were manufactured. Table 2 summarizes the samples and their notation.

2.5. Composite characterizations

2.5.1. X-ray tomography imaging

In order to visualize porosity and fibers inside composites, X-ray tomography was performed. A piece of each type of composite was cut into the laminate (3 mm^2 of section) with fibers in the length direction.

These samples were placed on a rotation stage within a X-ray microtomograph (Nanotom 180 XS, GE, Wunstorf, Germany). During the analysis, the X-ray detector was placed at 200 mm from the X-ray source (60 kV and 240 µA), and the distance between the source and the sample was adjusted to 5 mm to ensure maximum magnification while covering their entire cross-section. Thus, 2000 images were acquired during the 360° rotation of the sample. Each projection was averaged over 4 records of 1s each to reduce the noise level.

Once the scan was completed, a 3D reconstruction with a spatial volume resolution of 0.625 x 0.625 × 0.625 µm^3 per voxel was performed. In order to optimize the image analysis process, on each sample 8 vol of interest with a size of 0.75 × 0.75 × 1 mm^3 were defined. Then,

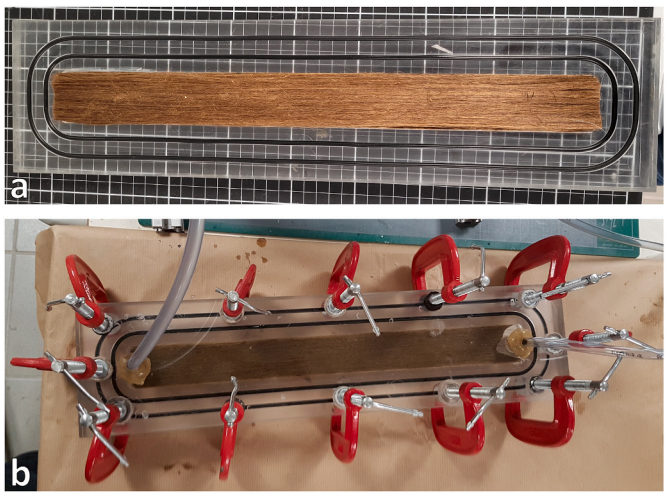

Fig. 2. a) Fiber placement within the mold; (b) infusion process.

Table 2
Sample nomenclature.

Reinforcement	Matrix	1050	InfuGreen
Raw fibers		1050-R	I–R
Torrefied fibers		1050-T	I-T
Fluorinated fibers		1050-F	I–F

to identify porosity and fibers inside the material, a pre-processing based on an automatic learning for image analysis has been performed using the Ilastik software. The process realized is an adaptation of the work of Berg et al. [60]. Then, a filter was used to smooth the noise of the images. Finally, the image was segmented in order to identify the presence of cavities within the overall composite, but also at the interface of the fibers.

Once the computer processing achieved on all 2000 images of each of the 8 zones of each sample, a 3D representation was made using the VGStudio Max© software (Volume Graphics, Heidelberg, Germany). More explanation and illustration of this procedure is presented in Supporting Information.

2.5.2. Tensile test

To evaluate the impact of the two treatments on the tensile properties of manufactured composites, tensile tests were performed according to ASTM D3039/D3039 M standard [61]. Six 170 × 15 × 3 mm^3 rectangular specimens with fibers oriented at 0° were cut from composite plates and tests were carried out on a Zwick UTS20K machine equipped with a 20 kN capacity load cell, at a crosshead displacement rate of 1 mm/min. Sample gauge length was fixed at 90 mm, and elongation of the tested composites was measured using a clip-on extensometer.

2.5.3. Three-point bending test

Flexural properties of bio-based composites have been investigated *via* three-point bending test, conducted following ASTM D790-03 [62] (however, only 4 samples were tested instead of 5 required by the standard, because of the limited amount of fibers available to manufacture composites). Sample dimension was 120 × 18 × 3 mm^3, and as the standard requires a span-to-depth ratio larger than 16:1 at minimum, and recommends it higher than 32:1, support span has been set to 100 mm (span-to-depth ratio = 33:1). Tests were carried out on a Zwick UTS20K machine equipped with a 20 kN capacity load cell, at a crosshead displacement rate of 1 mm/min.

2.5.4. Charpy impact test

Charpy impact strength of composites has been investigated using a pendulum impact tester ZwickRoell HIT50P with an impact tester of 50 J and the experimental procedure was defined to follow the NF EN ISO179-1 standard [63]. For long-fiber-reinforced materials, standard specimen dimensions are not specified (except for the sample thickness which is standardized at 3 mm), and only the ratio of the span between the specimen supports to the specimen dimension in the direction of the blow is imposed. According to the standard, our specimen if of "type 2". For this kind of sample, a span-to-length ratio of 20/25 (=0.8) is required. Therefore, Charpy flatwise impact specimens have been cut to the following dimensions: 50 × 10 × 3 mm^3, with a span of 40 mm (span-to-length ratio = 40/50 = 0.8). Unnotched specimens were tested in the normal direction (as recommended by the standard) and 6 samples were tested, because the coefficient of variation has a value of less than 5 %, (which allows to reduce the minimum number test specimens to five).

Charpy impact strength a_{cU} was calculated using equation (3)

$$a_{cU} = E_c / h \times b \quad (3)$$

where E_c (J) is the corrected energy absorbed by breaking the test specimen, h (mm) the specimen thickness, and b (mm) the specimen width.

2.5.5. Fracture surface observation

Fracture surfaces of tensile and bending specimens have been observed by Scanning Electron Microscope (SEM) at 100× of magnification (Zeiss Supra 55VP equipped with a Gemini column). To perform these observations, specimens were tilted with respect to the incident electron beam.

3. Results and discussion

3.1. Treatments

3.1.1. Homogeneous fluorine grafting

Considering the reactivity of F_2 gas, the tubular geometry of the reactor with a gas injection on one side and the pilot scale of the reactor (50 L), the first parameter to study is the homogeneity of the treatment. Thereby, the distribution of fluorine atoms on the fibers was studied as a function of both the tray on which the fibers were located and the distance with F_2 injection point.

FT-IR and ^{19}F NMR spectra of fluorinated flax fibers as a function of the location of the reinforcement within the reactor were acquired from samples collected at 10 cm and 65 cm from the edge, in the center of the fiber width (the 0 cm side corresponding to the width closest to the fluorine injection) on the 4 trays that were stacked in the reactor (Fig. 1b). These spectra are provided in supporting information in Figs. SI–4. In addition, XPS spectra of the fluorinated fibers (Figs. SI–5) were acquired at different positions of the fiber tapes at 0 cm, 32 cm and 65 cm from the edge, in the middle of the width (Figs. SI–5b Figs. SI–5c and Figs. SI–5d respectively, the 0 cm side being the closest to fluorine injection).

The presence of a signal on ^{19}F NMR spectra and the appearance of a peak at 688eV on F1s XPS spectra after fluorination of fibers highlight the covalent grafting of the fluorine atoms on the flax fiber surface. In addition, 5 contributions of C–F groups appeared in XPS on the C1s spectrum, which is an additional proof of grafting. Details on both peak assignments and the fluorination mechanisms are available in Ref. [45].

By comparing the set of FT-IR and ^{19}F NMR spectra, the quasi overlapping of the spectra, whatever the position of the sample in the trays (10 or 65 cm), coupled with the perfect similarity of these spectra between 10 and 65 cm, evidences that the fluorination treatment is chemically and quantitatively almost identical whatever the tray under study. In addition, considering now the deconvolution of the C1s spectra, a strong similarity between them is evidenced, proving that the grafted fluorinated species are nearly identical on the whole length of the tray. Furthermore, thanks to the global XPS survey, the atomic percentage of fluorinated groups present on fibers surface can be quantified (Table 3). Whatever the observed area, the values are almost identical, with a surface that contains 15 % CF, 5 % O-CF, 10 % CF_2 and 3 % CF_3 for a total of 33 % of fluorinated groups. Knowing that the fluorination treatment at a semi-pilot scale is achieved in a similar way on the whole fluorination reactor (between the 4 trays and on the whole length of these trays), on the surface (XPS) and deeper in the fibers (NMR and FT-IR), we could consider it as successfully realized and with the homogeneity well achieved.

Table 3
Percentage of carbon-based groups from XPS C1s spectra of raw and fluorinated flax fibers.

	Group relative content (%)				
	CF	O-CF	CF_2	CF_3	Total
Raw	0	0	0	0	0
0 cm	15	5.8	9.7	3.1	33.6
32 cm	17.6	5.2	9.4	2.5	34.8
65 cm	15.2	3.1	10.6	3.0	31.9

3.1.2. Homogeneous torrefaction

Torrefaction is a heat treatment similar to an incomplete pyrolysis of plants in an inert atmosphere [64], that allows the fiber polarity to be significantly reduced. If the impact of this treatment is difficult to quantify by conventional analysis techniques, color changes from brown to black occur in the 150°C–300 °C range [64]. Thereby, one of the easiest methods to evaluate the homogeneity (and the completion) of the treatment is to measure the changes of the fiber colors between different areas. Pictures of torrefied fibers have therefore been snapped on the 0–20 cm area of each tray (the 0 cm side corresponding to the side closest to the nitrogen injection), and on the whole length of the tray 2 (Fig. 1b). Thanks to computer software, the color of 25 areas randomly selected was identified in the CIE L*a*b* colorimetric representation. This large number of picked area was realized because of the natural intrinsically inhomogeneous color of raw fibers. Thus, reliable errors could be calculated to define whether or not the treatment is homogeneous. With the same aim, results were represented using box-and-whisker plot.

Fig. 3a displays the color difference between the different trays. Considering the uncertainties, a perfect similarity of L*, a* and b* values and then of color was evidenced. In the same way Fig. 3b also demonstrated that the fibers color is homogeneous on the whole length of the considered tray. Overall, this color homogeneity evidences that the torrefaction treatment has been applied homogeneously on all parts of the different treated fibers.

3.1.3. Impact of treatments

Before the manufacturing of eco-composites, the impacts of both homogenous fluorination and torrefaction treatments on the fiber properties have to be evaluated.

3.1.3.1. Modification of the surface energy. As demonstrated in a previous study [45], when controlled, fluorination treatment of flax fibers allows to modify their surface energy, by reducing their polar component (γ_s^p). On the other hand, the torrefaction treatment is also known to have a similar effect on the polar component of surface energy [11]. In order to identify and quantify modifications resulting from both treatments, tensiometric method was carried out and results are displayed on Fig. 4.

Before any treatment, raw flax fibers exhibit a high polarity of 19.1 $\pm$ 9 mN m^{-1}. After torrefaction and fluorination treatments, this polarity decreases to 6.0 $\pm$ 3.8 and 5.8 $\pm$ 2.4 mN m^{-1}, respectively. These close values will allow to compare treatment efficiencies on the composite mechanical properties, as close polar components should lead to similar

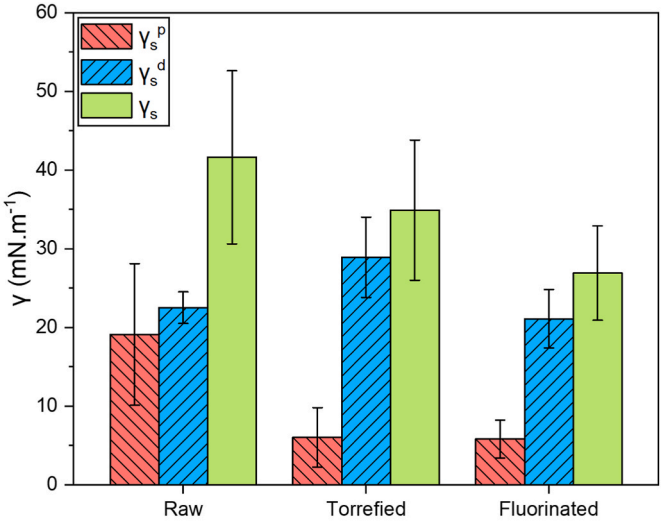

Fig. 4. Polar, dispersive and total surface energy of raw, torrefied and fluorinated flax fibers.

treated fibers/matrix compatibilities, which thus will no longer be an influent factor of this comparison.

On the other hand, we notice that the dispersive component remains nearly constant after the fluorination treatment. Knowing that the dispersive constant is related to the surface texture [37], the absence of changes may suggest the maintaining of the surface roughness during the fluorination treatment.

In addition, by comparing the standard deviation of the polar components of raw fibers and of treated ones, a reduction of these experimental uncertainties is achieved thanks to the fluorination. This phenomenon (also observed for fluorination at the laboratory scale) evidences that, when well controlled, fluorination and torrefaction treatments allow to limit the natural surface energy heterogeneity of vegetal fibers, making them of industrial interest.

The comparison of polarities of our treated fibers and different polymer matrix commonly employed for composite manufacturing such as epoxy ($\gamma_s^p \approx 5$ mN/m, depending on the formulation [46]), polyethylene ($\gamma_s^p \approx 0$ mN/m [65]), polypropylene ($\gamma_s^p \approx 0$ mN/m [65]) or poly(β-hydroxybutyrate) (PHB) ($\gamma_s^p \approx 11.5$ mN/m [66]) evidences that the fluorinated and torrefied flax fibers are highly compatible with epoxy matrix due to the modification of the surface properties. Thereby, epoxy matrix was employed to manufacture our composites. It is

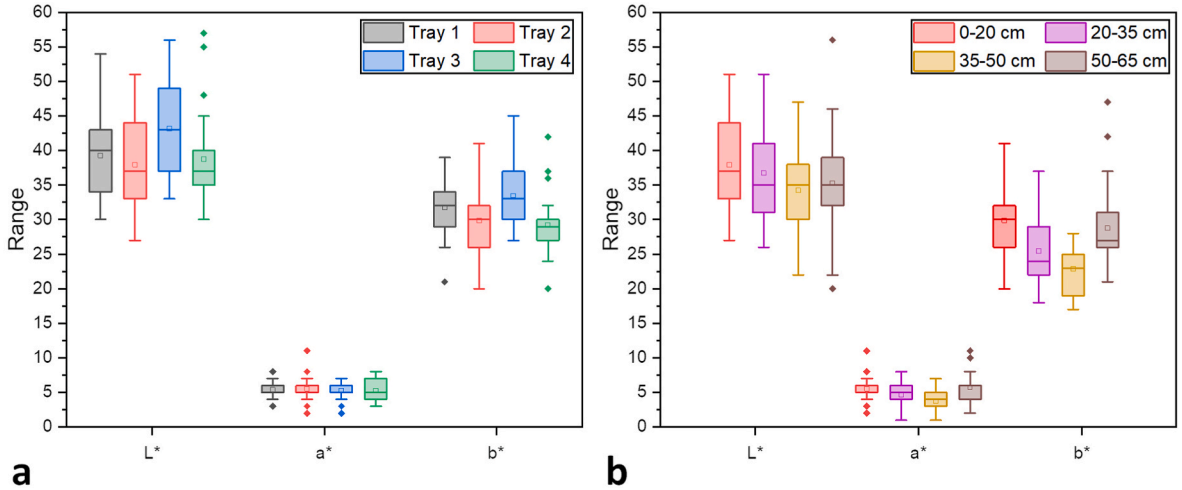

Fig. 3. L*, a* and b* components of color of torrefied fibers (a) between the 4 trays and (b) on the whole length of tray 4. (For interpretation of the references to color in this figure legend, the reader is referred to the Web version of this article.)

possible to note that the versatility of the fluorination treatment, thanks to the control of the duration, temperature, gas flow, dilution with an inert gas, allows the polarity of the fiber to be tailored to an "hydrophobic" polymer matrix.

3.1.3.2. Mechanical properties. Table 4 displays the tensile properties of raw and treated fibers. Both treatments affect the mechanical properties of the fibers in different manners. Where the torrefaction decreases the fiber Young's modulus (E), fluorination allows the material stiffness to be maintained. Moreover, where the maximum tensile stress (σ_m) and the elongation at break (A%) are both decreased by about 60 % after torrefaction, fluorination results in a decrease of the parameters by "only" about 30 %. All these observations are made without taking into account the experimental errors which are more due to the natural heterogeneity of flax fibers [67]. Therefore, it is clearly observed that the fluorination treatment has a moderate effect on fiber mechanical behavior, contrary to torrefaction which is well known to drastically reduce their tensile properties [19]. An explanation to this phenomenon relies to the fact that Young's modulus reflects volume properties of the material while ultimate tensile strength and maximum of elongation are more related to surface properties. Fluorination acts a surface treatment that does not affect bulk; so there is no reason for it to impact Young's modulus. However, surface modification and defaults generated by the fluorination treatment on the fiber surface induce a decrease of the properties at rupture, *e.g.* ultimate tensile strength and maximum of elongation [58]. According to Liotier et al. [19], the reduction of fiber polarity should allow a better fiber/matrix compatibility and thus an increase of the mechanical properties of the resulting composites, even if vegetal fibers have been embrittled by a treatment. In other words, the lower the polarity of fibers, the higher the improvements of the mechanical properties of the composite thus formed (as long as the polymer polarity stays below the fiber one) [19]. Such an enhancement can be achieved only if the intrinsic mechanical properties of the fibers are maintained or at least with moderate decrease; this is not the case after torrefaction, with more than 50 % decrease of σ_m and a 40 % decrease of A% contrary to fluorination.

3.2. Composites

Now that the effects of fluorination and torrefaction on individual flax fibers are known, the fabrication of composites from these raw fibers and their treated counterparts are presented. The goal here is to identify the advantages and disadvantages of such modifications on the final porosity and mechanical performance of the composite.

3.2.1. Porosity measurement

X-ray tomography was carried out in order to visualize fibers and porosity within the composite thanks to a 3D reconstruction of 8 vol of 1 mm^3 each made for the 3 types of composites. For each sample, one of the volumes is shown in Fig. 5 with a threshold revealing only flax fibers within the composite (Fig. 5a–c and e) and a threshold revealing only porosities (Fig. 5b–d and f).

Using these images, an Artificial Intelligence (AI) [60] was able, after a training, to identify and quantify all pixels that correspond to porosity inside the composite (Fig. 6a). Comparing first the 1050-R and 1050-F samples, it appears that the overall porosity present in the fluorinated-flax fiber reinforced material is significantly lower than the one present in the raw-fiber reinforced one. This fact evidences that fluorination treatment allows flax fibers to be compatibilized with the 1050 polymer matrix, thus reducing the porosity rate within the composite.

Furthermore, we were able to isolate the porosities present at the fiber/matrix interface using AI (Fig. 6b). Once again, we notice that the porosity rate at the interface is significantly lower for the fluorinated flax fiber-based composite.

For the case of the composites reinforced by torrefied flax fibers, the results (Fig. 6a and b respectively for the global porosity and the interface porosity) evidence a significant increase of the porosity rate within the composite. This phenomenon, in contradiction with the expected results and the observation of Pucci et al. [11] may have two origins: either the 2 mm^3 area analyzed was not representative of the overall composite or the torrefaction treatment would decompatibilize flax fibers with the 1050 matrix for an unknown reason in the present case. Even though it should be noted that many differences exist between this study and the one described in the paper [11], such as the fact that their fibers were a fabric and not 1D fibers, differences in resins, differences in operating conditions, etc., we should still have obtained a similar trend. Because of literature results [11] and the large standard deviation observed in Fig. 6a and b for the torrefied fibers, we favor the fact that the measurement area might not have been representative. The other hypothesis cannot be excluded yet, but the results of mechanical tests should allow a better understanding of the actual phenomenon.

In addition, still using AI, we were able to identify the composite fiber content (Table 5). Results show that all composites have a reinforcement rate in between 20 and 30 %. It is possible to note that the reinforcement rate has a high variability, due to the intrinsic heterogeneity of the natural fibers. The slight decrease observed in the fiber content for the 1050-F composite will be considered as non-significant, especially considering that 6 plies of fibers were introduced in each case, leading to a theoretically identical quantity of fibers, because our FlaxTape™ fabrics are calibrated at 110 g/m^2. The difference is more due to the limited area investigated than to any real difference. The reinforcement rate of our composites is estimated at around 25 % (V/V).

3.2.2. Effect of treatments on mechanical properties of composite

The next section aims to establish how the polarity decrease of flax fibers (inducing a better compatibility with hydrophobic polymer matrices such as epoxy) and the reduced porosity (a consequence of the enhanced compatibility) act on the composite mechanical properties using tensile tests, bending tests and Charpy impact tests.

3.2.2.1. Tensile test. Tensile tests are the most traditional and commonly used tests to evaluate the mechanical performance of materials. Results are respectively presented in Fig. 7a for composites based on 1050 resin and Fig. 7b for those made from Infugreen resin. Strain-Deformation curves are presented in Supporting Information (Figs. SI–5 & SI-6). Whereas the Young's modulus (E) remains almost constant after both fluorination and torrefaction, properties at break of the composites (ultimate tensile strength σ_m and maximal elongation A %) are decreased by both treatments, but not to the same extent.

Indeed, fluorination decreases the mechanical performance of the final composite to a much lesser extent than torrefaction.

- Concerning σ_m, we observe a decrease of more than 50 % for the torrefied fiber-based composite (~60 % and ~50 % for 1050-T and I-T, respectively, compared to I-Raw) against a 25 % decrease for fluorinated fiber-based composite.
- A% is decreased by 50 % for 1050-T and I-T, versus 11 % and 17 % for 1050-F and I–F composites, respectively.

By comparing these results with the mechanical properties observed on single fiber tests (Table 4), we clearly observe a similarity of evolution. Indeed, tensile tests on composites and on single fibers, both

Table 4
Evolution of fiber tensile properties depending on the applied treatment.

	Raw	Torrefied	Fluorinated
E (GPa)	37.5 ± 15.3	31.5 ± 13.9	36.1 ± 19.2
σ_m (MPa)	780 ± 423	279 ± 147	498 ± 284
A% (%)	1.95 ± 0.61	0.80 ± 0.37	1.35 ± 0.5

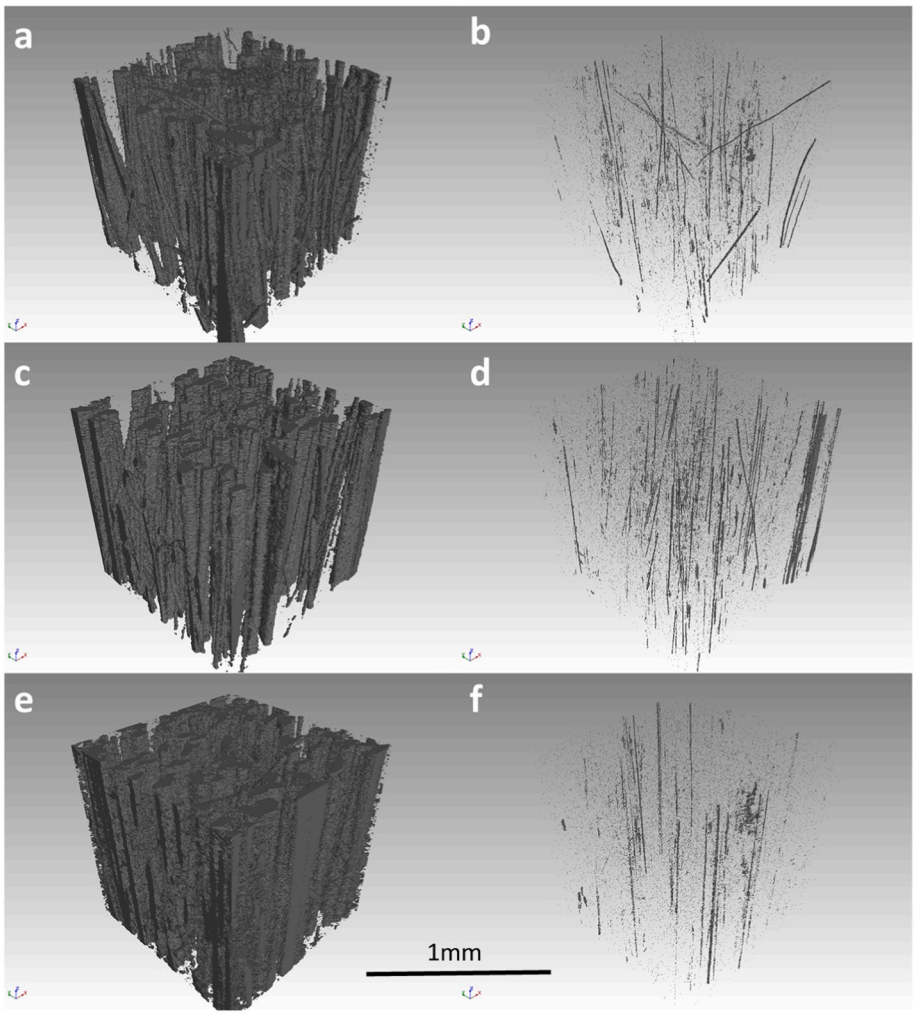

Fig. 5. 3D reconstruction and visualization of fibers and micrometric pores for raw (a and b respectively), torrefied (c and d respectively) and fluorinated (e and f respectively) flax fibers reinforcing the 1050-1056S epoxy resin.

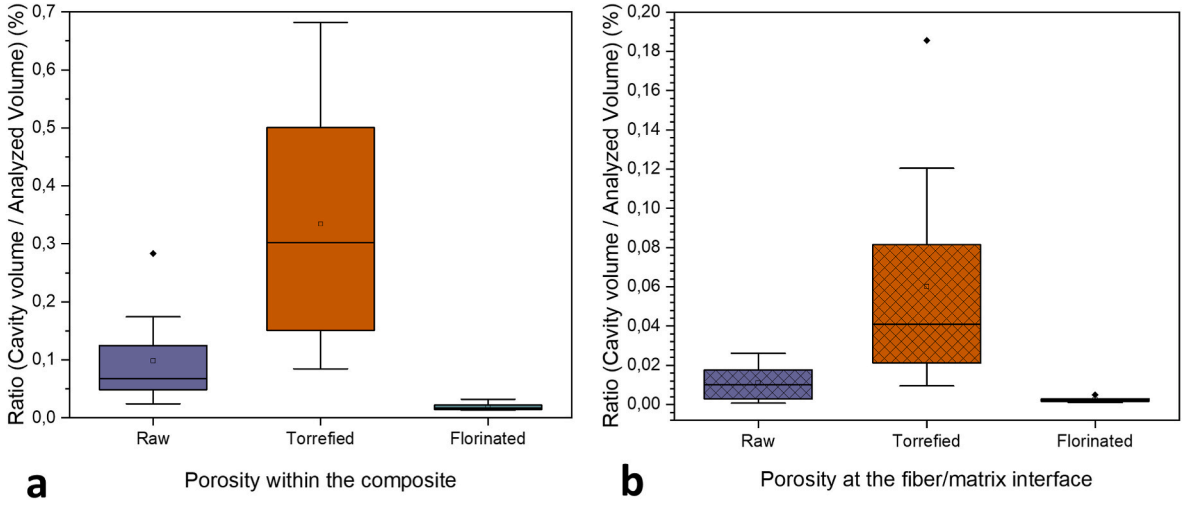

Fig. 6. Porosity rate (a) within the composite and (b) at the fiber/matrix interface; composite with 1050 resin.

highlight a conservation of the Young's modulus whatever the treatment. However, a drastic decrease of the "at break" properties of torrefied fibers and derived composites is observed while fluorinated samples (fibers and composites based on fluorinated fibers) exhibit a moderate decrease.

It is commonly admitted that the mechanical properties of a composite material are, on the one hand, related to the mechanical performance of the reinforcements and, on the other hand, correlated to the

Table 5
Percentage of the volume occupied by fibers in the composite.

1050-R	1050-T	1050-F
29.6 ± 6.6 %	27.3 ± 1.8 %	19.4 ± 7.6 %

quality of the interface between the fiber and the matrix. With high quality, this interface allows the load between reinforcements to be correctly transferred. However, considering our results, we suppose that there is a preponderance of one or another of these parameters depending on the deformation mode.

Since during tensile test, stress is applied parallel to the fibers direction (0° tension), the mechanical performance of the composites was mainly related to the mechanical performance of the fibers themselves. However, the latter was reduced by the torrefaction and fluorination treatments, in spite of the compatibility improvement between the fibers and the matrix, the reduction of the “at break” properties reduces in a parallel way (and in a similar order of magnitude) the mechanical properties of composites in tension.

In order to observe composite fracture surfaces, observations of post-rupture specimens from a macroscopic point of view (Figs. SI–7) as well as SEM observations were carried out and are presented in Fig. 8. In addition, higher magnification of the picture presented in Fig. 8 are also presented in Figs. SI–8.

From a macroscopic point of view, the observation of the I–R specimens (Figs. SI–7a) seems to show a fiber pull-out rupture. Indeed, impact of fibers on the fracture site can be distinctly observed and these latter are still relatively long. This suggests a rupture of the fiber/matrix interface; the interface thus acts as the limiting element which is at the origin of the composite failure, evidencing a limited compatibility. On the other hand, the I-T and I–F composites show a fracture surface that highlights a fiber breaking rather than their pull-out rupture. The limiting element is not the interface but the fibers themselves, as evidence of a better adhesion between the treated fibers and the matrix (compared to the raw fiber/epoxy combination).

These phenomena are also confirmed by the SEM images (Fig. 8). For 1050-R and I–R composites, the fiber pull-out effect is unambiguously observed because of the numerous long single fibers. Moreover, no trace of resin on their surface is present on the rupture area. The image for 1050-R evidences numerous "holes" from which raw fibers have been debonded, in good accordance with a fiber pull-out. 1050-T, 1050-F, I-T and I–F composites exhibit shorter fibers than those observed on the raw fiber composites. Moreover, these fibers are mainly observed in clusters with residual resin on their surface. This cohesive state after breaking can be reached only because the treated fibers are efficiently covered by the matrix. The absence of holes and the presence of pronounced breaks in the resin (especially in the image corresponding to the I-T specimen) are two other proofs of the absence of fiber pull-out.

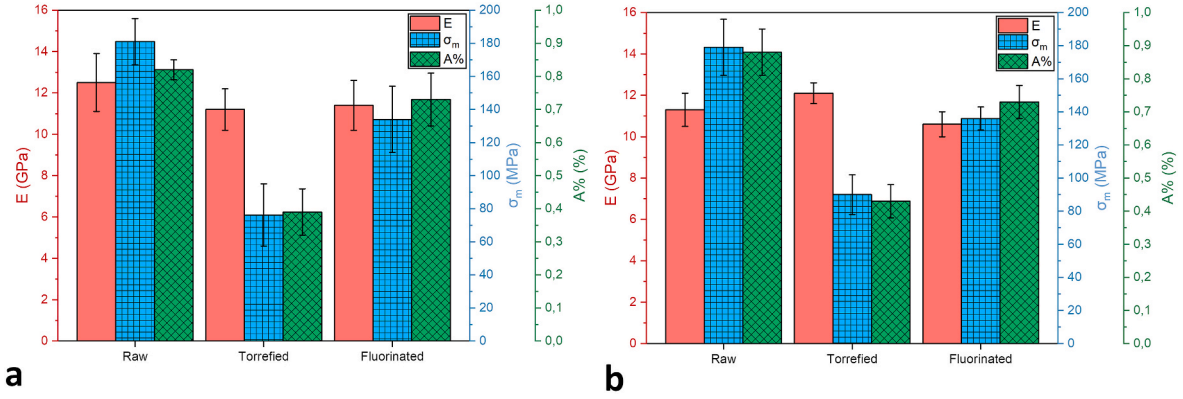

Fig. 7. Evolution of the (a) 1050 and (b) Infugreen resin-based composite mechanical properties depending on the treatment (E = Young’s modulus; σ_m = Ultimate tensile strength; A% = maximal elongation).

Fig. 8. SEM images of fracture surface of specimens after tensile tests.

To summarize the tensile test observations, Young's modulus remains constant regardless of the treatment performed on the fibers. On the contrary, both torrefaction and fluorination treatments of flax fibers decrease the "at break" mechanical properties of composites made from these treated reinforcements. This decrease is moderate for fluorination. This phenomenon evidences, at this stage, the superiority of the fluorination treatment compared to the torrefaction one. These evolutions can be explained by the fact that, during a tensile test performed in the fiber direction, the mechanical performances of the composites are mainly related to the mechanical performances of the fibers themselves. Consequently, since these treatments lowered the mechanical properties (σ_m and A%) of the fibers (Table 4), they also lowered the composite ones.

Nevertheless, observations of fracture surfaces allowed to demonstrate that matrix adhesion to the fibers was improved with both the torrefaction and fluorination treatments, thanks to the absence of fiber pull-out effects.

Therefore, if these results do not show the expected improvements in mechanical properties, it has to be remembered that even though tension remains the most common technique to measure the mechanical performance of a material, technical parts are often solicited under various modes (bending, compression, etc.). The effects of the treatments cannot be evaluated only by tensile tests, which have to be completed by other mechanical characterizations. Tests leading to higher fiber/matrix interface solicitation than tensile mode may be carried out.

3.2.2.2. Flexural test. Whether in 3 or 4 points configuration, flexural test induces strong shear stresses within the specimen, leading to a load transfer between the different reinforcements of the composite through the matrix. It should be noted that in a 3-point bending test, shear stress is present in the whole volume of the specimen, except on the area of the specimen located under the central loading nose which is in pure bending. In 4-point bending, the whole specimen volume located between the 2 loading noses is in pure bending, while the 2 external zones are solicited in shear stress. Therefore, flexural tests could highlight interesting properties of composites integrating fluorinated and torrefied fibers. Composites were thus analyzed in 3-point bending test in order to stress the interface as much as possible and evidence an eventual improvement of the composite mechanical performance.

By focusing first on the 1050 resin based-composites (Fig. 9a), a clear improvement of the flexural modulus (E_f) is observed for treated fibers (respectively by 10 % and 25 % for torrefied and fluorinated fibers). Regarding the flexural strength (σ_{fM}), results evidence a 10 % increase for the composites based on fluorinated fibers (1050-F), whereas the ones reinforced with torrefied fibers (1050-T) present a more than 30 % decrease of the σ_{fM} value compared to those based on raw flax fibers. Finally, both composites reinforced with treated reinforcements evidence a decrease in the percentage of maximum elongation (A%). However, this decrease is much more moderate in the case of fluorinated fibers reinforced composites (15 % decrease for 1050-F) than the one observed for composites reinforced with torrefied fibers (~50 % decrease for 1050-T). These evolutions therefore highlight a material stiffening following the fiber fluorination and torrefaction treatment, for the 1050 matrix-based composites. It should be noted here that the changes described above are out of uncertainty bars, evidencing significant evolutions.

Therefore, results highlight the interest of the fluorination treatment, since torrefaction has been much less efficient for improving the interfacial compatibility of eco-composites. Moreover, fluorination also increases composite σ_{fM} in contrast with the torrefaction and allows a more limited decrease of the maximum deformation percentage. This phenomenon can be explained by observing the mechanical characteristics of torrefied and fluorinated single fibers. Indeed, if the 2 treatments allow to decrease the polarity of the fibers in an equivalent way (Fig. 4), as torrefaction acts on the whole volume, it weakens significantly the flax fiber mechanical properties whereas fluorination, by only modifying the outmost surface of reinforcements, allows a better preservation of fiber mechanical performances.

The same behavior can be observed with Infugreen-based composites. Indeed, after fluorination and torrefaction treatments, flexural modulus of the composites is increased compared to the composites with raw fiber reinforcement. On the other hand, the percentage of maximum deformation at break of the composite decreases after the treatment (slightly for the fluorinated fibers-based composites and significantly for the composites reinforced with torrefied fibers). A stiffening of the composites with both fiber treatment is then noted. In addition, unlike the results obtained with the 1050 resin-based composites here, σ_{fM} decreases for both I–F composite as well as for I-T composite. However, it should be noticed that this decrease is much more moderated for fluorinated reinforcements (~10 %) than for torrefied ones (~35 %).

The results obtained with 1050 and Infugreen resins converge on the fact that flexural modulus is improved by fiber fluorination and torrefaction. However, here the improvement in the flexural modulus of I-T and I–F is less clear than that previously observed for composites based on 1050 resin. Indeed, for the Infugreen-based composites, the high uncertainty in the flexural modulus of the I-T composites and the more moderate improvement of the fluorinated fiber composites show an overlap of the experimental uncertainty bars (slight between I–R and I–F and total between I–R and I-T).

This moderate increase in mechanical behavior can be explained by comparing the surface energy of both resins and fibers. Indeed, Table 1 indicates that the uncured 1050 resin exhibit values of γ_s^p and γ_s^d of 5.5 mN/m and 26.4 mN/m, respectively, while the Infugreen has a polar component γ_s^p measured at 0 mN/m and γ_s^d equal to 46.7 mN/m. Our fibers, whether fluorinated or torrefied, have a polar component γ_s^p

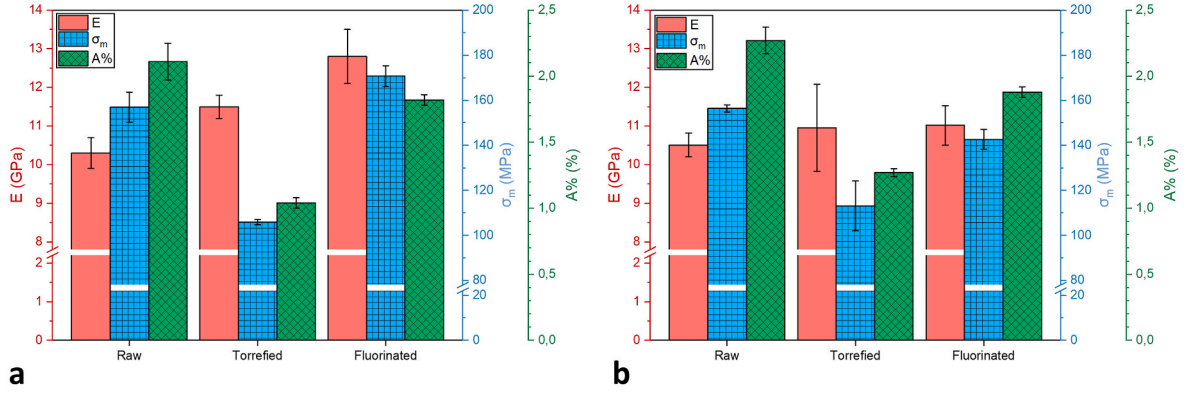

Fig. 9. Evolution of the (a) 1050 and (b) Infugreen resin-based composite flexural properties depending on the treatment (E = Flexural modulus; σ_m = Flexural strain at break; A% = percentage of maximal elongation).

measured around 6.0 mN/m. Thereby, the polarity of these treated fibers fits perfectly with the polarity of the 1050 resin and less with Infugreen, explaining the differences in favor of 1050.

As for tensile tests, a post-rupture examination was performed from a macroscopic point of view and by SEM, respectively presented in Figs. SI–9 (in supporting information) and Fig. 10 (Higher magnification of SEM picture are also presented in Figs. SI–10).

From a macroscopic point of view (Figs. SI–9), we notice that the composites reinforced with torrefied flax fibers (Figs. SI–9b) broke at the end of the test, while the composites reinforced with raw flax fibers (Figs. SI–9a) and fluorinated flax fibers (Figs. SI–9c) bent but did not break completely. This can be explained by the fact that the torrefied fiber composites have a much lower σ_{fM} than the 2 other ones. Furthermore, we also notice that the fluorinated fiber composite specimens (Figs. SI–9c) have, post-test, a higher "bending angle" than the raw fibers one because of the stiffening of the fluorinated flax fiber composites compared to the raw fiber composites, previously discussed.

About the fracture surfaces investigated by SEM (Fig. 10), we observe the same phenomena as those previously observed on the post-tension specimens. Indeed, picture on the post-bending specimens of the raw fibers composites (1050-R and I–R) show a fiber pull-out effect which is highlighted by the presence of long fibers without resin on their surface as well as small holes present on the rupture zone. On the other hand, fibers present in the 1050-T, 1050-F, I-T and I–F composites are mainly observed in clusters and with resin residue on their surface. This demonstrates once again a better fiber/matrix compatibility between the epoxy and the torrefied/fluorinated flax fibers.

To conclude, results clearly evidence that fluorination and torrefaction treatments allow to enhance the flexural modulus of specimen but on the other hand, decrease the maximum elongation. A composite stiffening is achieved thanks to reinforcement fluorination/torrefaction. It also can be noticed that the flexural modulus enhancement is higher and the maximum elongation decrease is lower with fluorination than with torrefaction. In addition, because of the closer polar components γ_s^p of treated fibers with uncured 1050 resin than with uncured Infugreen one, the improvement of the composite flexural properties is higher with the 1050 polymer matrix.

3.2.2.3. Charpy impact test. Another characteristic often measured to qualify a material is its capacity to absorb a shock. In order to quantify this ability on the studied materials, Charpy impact test was performed.

Results are presented in Fig. 11a. A similar behavior is observed for both matrices according to the type of reinforcement employed. In both cases, composites reinforced by raw fibers have the best impact resistance with an absorbed energy of about 25 kJ/m^2. Composites reinforced by fluorinated flax have lower impact energy (15–20 kJ/m^2, depending on the resin used), while composites made from torrefied flax fibers have the lowest impact properties (5–10 kJ/m^2).

In addition to these results, Fig. 11b shows pictures of the post-impact specimens for the Infugreen-based composites, but the same phenomena are observable for those based on 1050 resin. Pictures reveal that whereas the torrefied or fluorinated flax-based composite specimens present a complete failure, raw flax-based specimens show only partial failure. This fact, in addition to the higher a_{cU} of raw fiber-based composite demonstrate that raw flax provides a better absorption capacity to the composite than treated flax fibers. This phenomenon can be explained by the stiffening of the composites inherent to the treatment of the fibers previously observed during the flexural tests. Indeed, by becoming stiffer, the composites have lost in resilience capacity and their ability to absorb shock.

Nevertheless, by comparing both treatments, we clearly observed that the fluorinated fiber-based composite better absorb energy than those reinforced with torrefied fibers. Once again, the higher interest of the fluorination treatment is demonstrated.

3.2.2.4. Discussion. To compare the impact of torrefaction and fluorination treatments on mechanical properties of composites made from these reinforcements, three types of complementary mechanical tests were carried out. First, tensile tests showed that Young modulus remains constant compared to composites reinforced with raw fibers, whatever the treatment of the fibers. On the other hand, the ultimate tensile strength and ultimate tensile elongation moderately decreased with fluorination and significantly with torrefaction. This evolution follows the behavior of single fibers in tensile tests. Indeed, since tensile test only lightly stressed the interface, the resulting mechanical behavior of composites is mainly related to the mechanical performances of the fibers and not on the fiber/matrix interface.

When a test that focuses more on the interface (such as 3-point bending) is implemented, a significant increase in the mechanical performance of composites made from treated reinforcements is observed, due to the improvement of the fiber/matrix interface linked to the decrease in internal porosity in the composite, highlighted by X-ray tomography. Indeed, an increase of the flexural modulus is observed whatever the treatment applied to the fibers. However, results show, on

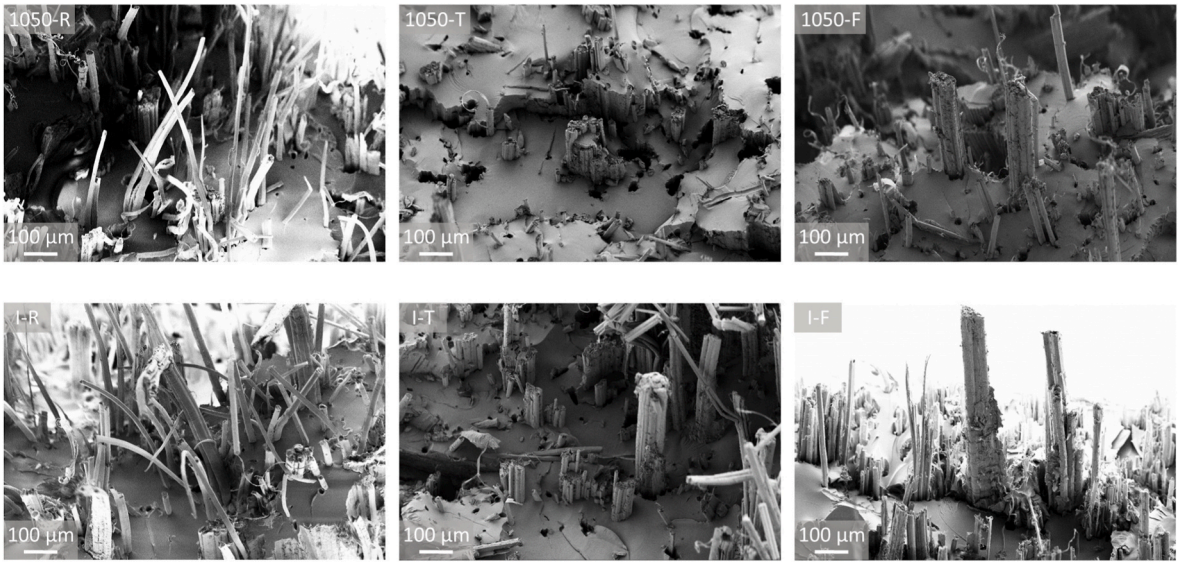

Fig. 10. SEM images of fracture surfaces of specimens tested in 3-point bending.

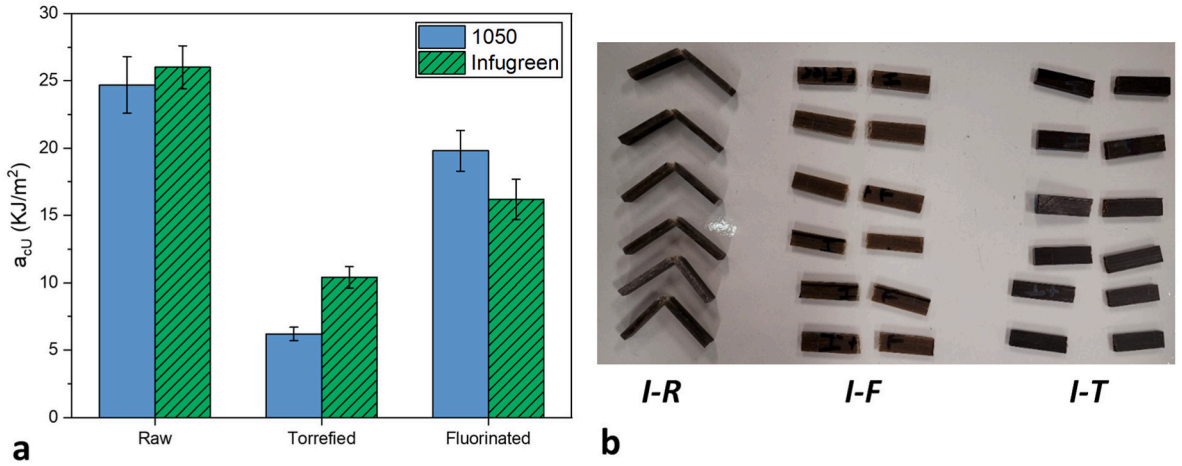

Fig. 11. (a) Charpy impact strength of composite specimens as a function of resin and reinforcement type; (b) picture of Charpy impact test specimen post-shock.

the one hand, that torrefaction, by embrittling the fibers much more than fluorination, leads to a more limited improvement of mechanical performances of the composites, but also that this improvement is strongly dependent on the proximity between polar ratios of the polymer matrix and of the fibers.

In addition, the increase in flexural modulus described above demonstrates a stiffening of the treated flax-based composites, resulting in a decrease in the resilience of these materials to various impacts.

It can be noted that the problem of fiber/matrix compatibility is more complex than summarized by Liotier et al. [19] "*since the wettability of fibres has been improved, the overall mechanical behaviour of composites manufactured by LCM is better with treated fibres*". All the stakes are linked to the nature of the stresses applied on a technical part. Therefore, for a part solicited under bending and whose resilience is only of secondary importance, compatibility treatments like fluorination appear very interesting. On the other hand, this type of modifications seems totally counter-productive for part subjected to tensile stress or requiring a high shock-absorption capacity. In addition, other parameter like fiber volume fraction, resin type, manufacturing process, etc. also vary the impact rate of the compatibility treatment.

In any case, compared to torrefaction, flax fluorination allows, whatever the mode of solicitation, good mechanical performances to be achieved, demonstrating its interest for the manufacture of eco-composites. All these conclusions are highlighted in Fig. 12. Indeed, we clearly observe that 1050-T composites are in every way outperformed by 1050-F composites. However, between the 1050-R and the 1050-F composites, it depends on the property studied.

It would be interesting to complete this study with other mechanical tests (fatigue, torsion, etc.) in order to perfectly characterize the composites based on treated flax fibers and to completely know their interests and their defects.

4. Conclusion

Based on the work previously carried out at a laboratory scale [45], transposition of the fluorination treatment of flax fibers to a semi-industrial scale has been successfully achieved. At this scale, fluorination allows to uniformly and covalently graft fluorine atoms on the flax fibers surface without degradation of the latter, in spite of the constraints induced (maximum gas flows and 50 L volume for the reactor) by the large dimensions of the fluorination reactor employed. Thanks to FT-IR, ^{19}F NMR and XPS analyses, it has been proved that the treatment was homogeneous on the whole of the 4 fibers trays present within the reactor, in spite of its large size (65 m long and 20 cm wide). This experimentation demonstrates that fluorination is perfectly achievable on an industrial scale for materials that are complex because

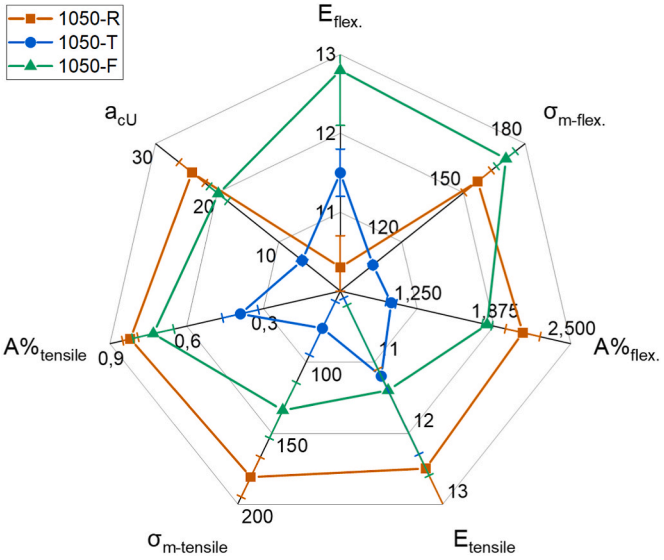

Fig. 12. Summary of the composite mechanical performances according to the reinforcement for the 1050 matrix.

of both their multi-component character and their reactivity as natural fibers. In addition, to bring a point of comparison to the fluorination of flax, torrefaction (known to reduce the polarity of fibers) was also conducted with the aim of obtaining torrefied fibers with the same polarity as fluorinated fibers. Therefore, fluorination and torrefaction result in a similar reduction of flax polarity from ~20 mN/m to ~5 mN/m. Fluorination equivalently reduces the polarity of flax fibers than torrefaction but with less damage of the single fiber mechanical performance. As a matter of fact, whereas torrefaction treatment decreases the ultimate fiber tensile strength (σ_m) and percentage of maximum elongation (A%) by ~60 %, fluorination decreases them by ~30 % only.

Using tensile tests on composites made with the raw and treated fibers, a stability of Young modulus was observed whatever the treatment applied to the fibers. However, ultimate tensile strenght (σ_m) and percentage of maximum elongation (A%) of composites decreased in a moderate way with fluorinated fibers and more significantly with torrefied fibers.

3-point bending tests reveal a 30 % increase in the flexural modulus of the composite reinforced with fluorinated flax fibers. Torrefied fiber-based composites also show a flexural modulus increase, but only by 10 %, because of the embrittlement of the fibers during the torrefaction.

However, in both cases this stiffening decreases the resilience of the composites based on treated reinforcements.

The interest of the compatibilization treatment depends then on the mode of solicitation of the technical part which is going to be designed. In any case for natural filler, fluorination has to be preferred as compatibilization treatment because it induces higher mechanical performances in flexural mode and more moderate decreases in tensile and Charpy impact tests. In addition, counter-performances through tensile solicitation may be counter-balance using hybrid composite as employed by several authors (for example [5,6]).

In the context of this paper, we have investigated the effect of fluorination (and torrefaction as witness) treatment through the most standard mechanical tests and a correlation has been found between interphase solicitations and mechanical performances (*i.e.:* 3-points bending test in our case). Some other mechanical tests such as Short Beam Shear Test or 4 points bending test for example that are known to highly solicitate the interphase of composite would be able to achieve better understanding. In addition, it is important to remind that fluorination treatment was only partially optimized, therefore such better results are expected with an optimization of it.

In addition, it is important to underline the universality of the fluorination treatment for compatibilization with respect to the majority of dispersive matrix. While sizing treatment for example implies a specific sizing/matrix couple, the versatility of the fluorination process *via* the operating conditions (temperature, gas flow, duration, dilution, purge speed, …) can be used to tailor the polar ratio of the fiber and then adjusted to the one of the polymer, and this in a solvent-free process without environmental release, in good agreement with the concept of eco-composite.

CRediT authorship contribution statement

Olivier Téraube: Writing – original draft, Visualization, Validation, Software, Methodology, Investigation, Formal analysis, Data curation, Conceptualization. **Jean-Charles Agopian:** Writing – review & editing, Investigation, Formal analysis. **Monica Francesca Pucci:** Writing – review & editing, Validation, Resources, Methodology. **Pierre-Jacques Liotier:** Writing – review & editing, Validation, Resources, Methodology. **Pierre Conchon:** Software, Resources, Formal analysis, Data curation. **Éric Badel:** Writing – review & editing, Software, Resources, Formal analysis. **Samar Hajjar-Garreau:** Writing – review & editing, Resources, Investigation. **Honorine Leleu:** Writing – review & editing, Investigation, Formal analysis. **Jean-Baptiste Baylac:** Writing – review & editing, Investigation, Formal analysis. **Nicolas Batisse:** Writing – review & editing, Validation, Resources, Investigation. **Karine Charlet:** Writing – review & editing, Supervision, Resources, Project administration, Methodology, Conceptualization. **Marc Dubois:** Writing – review & editing, Supervision, Resources, Project administration, Methodology, Funding acquisition, Conceptualization.

Declaration of competing interest

The authors declare that they have no known competing financial interests or personal relationships that could have appeared to influence the work reported in this paper.

Acknowledgements

This work was financially supported by the Région Auvergne-Rhône-Alpes through the FLUONAT Project, and encouraged by Solvay Group Saint-Fons (France).

In addition, the authors would like to thank Alexis Gravier, Alexis Jean and Michel Drean from SIGMA-Clermont for their help during composite preparation and the realization of the mechanical tests.

Data availability

Data will be made available on request.

References

[1] Vinod A, Sanjay MR, Suchart S, Jyotishkumar P. Renewable and sustainable biobased materials: an assessment on biofibers, biofilms, biopolymers and biocomposites. J Clean Prod 2020;258:120978. https://doi.org/10.1016/j.jclepro.2020.120978.

[2] Baley C, Bourmaud A, Davies P. Eighty years of composites reinforced by flax fibres: a historical review. Compos Appl Sci Manuf 2021;144:106333. https://doi.org/10.1016/j.compositesa.2021.106333.

[3] Lotfi A, Li H, Dao DV, Prusty G. Natural fiber–reinforced composites: a review on material, manufacturing, and machinability. J Thermoplast Compos Mater 2021;34:238–84. https://doi.org/10.1177/0892705719844546.

[4] Mochane MJ, Mokhena TC, Mokhothu TH, Mtibe A, Sadiku ER, Ray SS, et al. Recent progress on natural fiber hybrid composites for advanced applications: a review. Express Polym Lett 2019;13:159–98. https://doi.org/10.3144/expresspolymlett.2019.15.

[5] Agopian J-C, Téraube O, Hajjar-Garreau S, Charlet K, Dubois M. Study of carbon-flax hybrid composites modified by fibre fluorination. J Fluor Chem 2023;272:110213. https://doi.org/10.1016/j.jfluchem.2023.110213.

[6] Ayyappan V, Tengsuthiwat J, Raghunathan V, Sanjay MR, Siengchin S. Quasi-static – cyclic and fatigue properties of carbon-innegra/pineapple multi-material laminates. Ind Crop Prod 2024;222:119894. https://doi.org/10.1016/j.indcrop.2024.119894.

[7] Célino A, Fréour S, Jacquemin F, Casari P. The hygroscopic behavior of plant fibers: a review. Front Chem 2014;1:1–12. https://doi.org/10.3389/fchem.2013.00043.

[8] Al-Oqla FM, Salit MS. Natural fiber composites. Materials selection for natural fiber composites. Elsevier; 2017. p. 23–48.

[9] Dhakal H, Zhang Z, Richardson M. Effect of water absorption on the mechanical properties of hemp fibre reinforced unsaturated polyester composites. Compos Sci Technol 2007;67:1674–83. https://doi.org/10.1016/j.compscitech.2006.06.019.

[10] Thakur VK, Thakur M, Kessler MR. Handbook of composites from renewable materials, vol. 4. Scrivener Publishing LLC; 2017.

[11] Pucci MF, Liotier P-J, Seveno D, Fuentes C, Van Vuure A, Drapier S. Wetting and swelling property modifications of elementary flax fibres and their effects on the Liquid Composite Molding process. Compos Appl Sci Manuf 2017;97:31–40. https://doi.org/10.1016/j.compositesa.2017.02.028.

[12] Chotirat L, Chaochanchaikul K, Sombatsompop N. On adhesion mechanisms and interfacial strength in acrylonitrile–butadiene–styrene/wood sawdust composites. Int J Adhesion Adhes 2007;27:669–78. https://doi.org/10.1016/j.ijadhadh.2007.02.001.

[13] Kazayawoko M, Balatinecz JJ, Matuana LM. Surface modification and adhesion mechanisms in woodfiber-polypropylene composites. J Math Sci 1999:6189–99.

[14] Klason C, Kubát J, Strömvall H-E. The efficiency of cellulosic fillers in common thermoplastics. Part 1. Filling without processing aids or coupling agents. Int J Polym Mat Po 1984;10:159–87. https://doi.org/10.1080/00914038408080268.

[15] Mburu F, Dumarçay S, Bocquet JF, Petrissans M, Gérardin P. Effect of chemical modifications caused by heat treatment on mechanical properties of Grevillea robusta wood. Polym Degrad Stabil 2008;93:401–5.

[16] Berthet M-A, Commandré J-M, Rouau X, Gontard N, Angellier-Coussy H. Torrefaction treatment of lignocellulosic fibres for improving fibre/matrix adhesion in a biocomposite. Mater Des 2016;92:223–32. https://doi.org/10.1016/j.matdes.2015.12.034.

[17] Podgorski L, Chevet B, Onic L. Modification of wood wettability by plasma and corona treatments. Int J Adhesion Adhes 2000:103–11. https://doi.org/10.1016/S0143-7496(99)00043-3.

[18] Lux C, Szalay Z, Beikircher W, Kováčik D, Pulker HK. Investigation of the plasma effects on wood after activation by diffuse coplanar surface barrier discharge. Eur J Wood Prod 2013;71:539–49. https://doi.org/10.1007/s00107-013-0706-3.

[19] Liotier P-J, Pucci MF, Le Duigou A, Kervoelen A, Tirilló J, Sarasini F, et al. Role of interface formation versus fibres properties in the mechanical behaviour of bio-based composites manufactured by Liquid Composite Molding processes. Compos B Eng 2019;163:86–95. https://doi.org/10.1016/j.compositesb.2018.10.103.

[20] Kabir MM, Wang H, Lau KT, Cardona F. Chemical treatments on plant-based natural fibre reinforced polymer composites: an overview. Compos B Eng 2012;43:2883–92. https://doi.org/10.1016/j.compositesb.2012.04.053.

[21] Zhou Y, Fan M, Chen L. Interface and bonding mechanisms of plant fibre composites: an overview. Compos B Eng 2016;101:31–45. https://doi.org/10.1016/j.compositesb.2016.06.055.

[22] Ichazo MN, Albano C, Gonza J. Polypropylene/wood flour composites: treatments and properties. Compos Struct 2001;54:207–14. https://doi.org/10.1016/S0263-8223(01)00089-7.

[23] Hassan A, Rahman NAbd, Yahya R. Extrusion and injection-molding of glass fiber/MAPP/polypropylene: effect of coupling agent on DSC, DMA, and mechanical

properties. J Reinforc Plast Compos 2011;30:1223–32. https://doi.org/10.1177/0731684411417916.
[24] Mohebby B, Fallah-Moghadam P, Ghotbifar AR, Kazemi-Najafi S. Influence of maleic-anhydride-polypropylene (MAPP) on wettability of polypropylene/wood flour/glass fiber hybrid composites. J Agric Sci Technol 2011;13:877–84.
[25] Dhilip JDJ, Raghunathan V, Mohan R, Ayyappan V, Rangappa SM, Siengchin S. Mechanical and flammability properties of ultrasonically processed silane-treated areca-banana fiber-reinforced epoxy composites for lightweight applications. Biomass Conv Bioref 2024. https://doi.org/10.1007/s13399-024-06124-w.
[26] Stamm AJ, Burr HK, Kline AA. Staybwood—heat-stabilized wood. Industrial and Engeneering Chemistry 1946;38:630–4. https://doi.org/10.1021/ie50438a027.
[27] Dong A, Fan X, Wang Q, Yu Y, Cavaco-Paulo A. Hydrophobic surface functionalization of lignocellulosic jute fabrics by enzymatic grafting of octadecylamine. Int J Biol Macromol 2015;79:353–62. https://doi.org/10.1016/j.ijbiomac.2015.05.007.
[28] Dong A, Yu Y, Yuan J, Wang Q, Fan X. Hydrophobic modification of jute fiber used for composite reinforcement via laccase-mediated grafting. Appl Surf Sci 2014;301:418–27. https://doi.org/10.1016/j.apsusc.2014.02.092.
[29] Fiore V, Scalici T, Nicoletti F, Vitale G, Prestipino M, Valenza A. A new eco-friendly chemical treatment of natural fibres: effect of sodium bicarbonate on properties of sisal fibre and its epoxy composites. Compos B Eng 2016;85:150–60. https://doi.org/10.1016/j.compositesb.2015.09.028.
[30] Gulati D, Sain M. Fungal-modification of natural fibers: a novel method of treating natural fibers for composite reinforcement. J Polym Environ 2006;14:347–52. https://doi.org/10.1007/s10924-006-0030-7.
[31] Huang X, Wang A, Xu X, Liu H, Shang S. Enhancement of hydrophobic properties of cellulose fibers via grafting with polymeric epoxidized soybean oil. ACS Sustainable Chem Eng 2017;5:1619–27. https://doi.org/10.1021/acssuschemeng.6b02359.
[32] Kick T, Grethe T, Mahltig B. A natural based method for hydrophobic treatment of natural fiber material. ACSi 2017;64:373–80. https://doi.org/10.17344/acsi.2017.3232.
[33] Lee K, Jur JS, Kim DH, Parsons GN. Mechanisms for hydrophilic/hydrophobic wetting transitions on cellulose cotton fibers coated using Al $_2$ O $_3$ atomic layer deposition. J Vac Sci Technol A: Vacuum, Surfaces, and Films 2012;30:01A163. https://doi.org/10.1116/1.3671942.
[34] Thakur K, Kalia S, Pathania D, Kumar A, Sharma N, Schauer CL. Surface functionalization of lignin constituent of coconut fibers via laccase-catalyzed biografting for development of antibacterial and hydrophobic properties. J Clean Prod 2016;113:176–82. https://doi.org/10.1016/j.jclepro.2015.11.048.
[35] Wang Q, Xiao S, Shi SQ, Xu S, Cai L. Self-bonded natural fiber product with high hydrophobic and EMI shielding performance via magnetron sputtering Cu film. Appl Surf Sci 2019;475:947–52. https://doi.org/10.1016/j.apsusc.2019.01.059.
[36] Kharitonov AP. Practical applications of the direct fluorination of polymers. J Fluor Chem 2000;103:123–7. https://doi.org/10.1016/S0022-1139(99)00312-7.
[37] Kharitonov AP, Simbirtseva GV, Tressaud A, Durand E, Labrugère C, Dubois M. Comparison of the surface modifications of polymers induced by direct fluorination and rf-plasma using fluorinated gases. J Fluor Chem 2014;165:49–60. https://doi.org/10.1016/j.jfluchem.2014.05.002.
[38] Kharitonov AP, Taege R, Ferrier G, Teplyakov VV, Syrtsova DA, Koops G-H. Direct fluorination—useful tool to enhance commercial properties of polymer articles. J Fluor Chem 2005;126:251–63. https://doi.org/10.1016/j.jfluchem.2005.01.016.
[39] Maity J, Jacob C, Das CK, Singh RP. Direct fluorination of Twaron fiber and investigation of mechanical thermal and morphological properties of high density polyethylene and Twaron fiber composites. J Appl Polym Sci 2008;107:3739–49. https://doi.org/10.1002/app.27510.
[40] Kharitonov AP. Direct fluorination of polymers. Nova Publishers; 2008.
[41] Pouzet M, Dubois M, Charlet K, Béakou A. From hydrophilic to hydrophobic wood using direct fluorination: a localized treatment. C R Chim 2018;21:800–7. https://doi.org/10.1016/j.crci.2018.03.009.
[42] Kharitonov AP, Kharitonova LN. Surface modification of polymers by direct fluorination: a convenient approach to improve commercial properties of polymeric articles. Pure Appl Chem 2009;81:451–71. https://doi.org/10.1351/PAC-CON-08-06-02.
[43] Agopian J-C, Teraube O, Dubois M, Charlet K. Fluorination of carbon fibre sizing without mechanical or chemical loss of the fibre. Appl Surf Sci 2020;534:147647. https://doi.org/10.1016/j.apsusc.2020.147647.
[44] Teraube O, Agopian J-C, Petit E, Metz F, Batisse N, Charlet K, et al. Surface modification of sized vegetal fibers through direct fluorination for eco-composites. J Fluor Chem 2020;238:109618. https://doi.org/10.1016/j.jfluchem.2020.109618.
[45] Téraube O, Agopian J-C, Pucci MF, Liotier P-J, Hajjar-Garreau S, Batisse N, et al. Fluorination of flax fibers for improving the interfacial compatibility of eco-composites. SMT Trends 2022;33:e00467. https://doi.org/10.1016/j.susmat.2022.e00467.
[46] Pucci MF, Liotier P-J, Drapier S. Tensiometric method to reliably assess wetting properties of single fibers with resins: Validation on cellulosic reinforcements for composites. Colloids Surf A Physicochem Eng Asp 2017;512:26–33. https://doi.org/10.1016/j.colsurfa.2016.09.047.
[47] CasaXPS version 2.3.18 (www.casaxps.com) [n.d].
[48] Rodríguez BA, Mendoza S, Iturriga MH, Castaño-Tostado E. Quality parameters and antioxidant and antibacterial properties of some Mexican honeys. J Food Sci 2012;77:C121–7. https://doi.org/10.1111/j.1750-3841.2011.02487.x.
[49] Larraín RE, Schaefer DM, Reed JD. Use of digital images to estimate CIE color coordinates of beef. Food Res Int 2008;41:380–5. https://doi.org/10.1016/j.foodres.2008.01.002.
[50] Gómez Polo C, Gómez Polo M, Montero J, Martínez Vazquez De Parga JA, Celemin Viñuela A. Correlation of natural tooth colour with aging in the Spanish population. Int Dent J 2015;65:227–34. https://doi.org/10.1111/idj.12176.
[51] Sgarbossa A, Costa C, Menesatti P, Antonucci F, Pallottino F, Zanetti M, et al. Colorimetric patterns of wood pellets and their relations with quality and energy parameters. Fuel 2014;137:70–6. https://doi.org/10.1016/j.fuel.2014.07.080.
[52] Pouzet M, Dubois M, Charlet K, Béakou A, Leban J-M, Bada M. Fluorination renders the wood surface hydrophobic without any loss of physical and mechanical properties 2019;133:133–41. https://doi.org/10.1016/j.indcrop.2019.02.044.
[53] Young T. An essay on the cohesion of fluids. Phil Trans Roy Soc Lond 1805;95:65–87.
[54] Schellbach SL, Monteiro SN, Drelich JW. A novel method for contact angle measurements on natural fibers. Mater Lett 2016;164:599–604. https://doi.org/10.1016/j.matlet.2015.11.039.
[55] Qiu S, Fuentes CA, Zhang D, Van Vuure AW, Seveno D. Wettability of a single carbon fiber. Langmuir 2016;32:9697–705.
[56] Hodzic A, Stachurski ZH. Droplet on a fibre: surface tension and geometry. Compos Interfaces 2001;8:415–25. https://doi.org/10.1163/156855401753424451.
[57] Van Hazendonk JM, Van der Putten JC, Keurentjes JTF, Prins A. A simple experimental method for the measurement of the surface tension of cellulosic fibres and its relation with chemical composition. Colloids Surf A Physicochem Eng Asp 1993;81:251–61.
[58] Téraube O, Agopian J-C, Pucci MF, Liotier P-J, Hajjar-Garreau S, Batisse N, et al. Fluorination of flax fibers for improving the interfacial compatibility of eco-composites. SMT Trends 2022:e00467. https://doi.org/10.1016/j.susmat.2022.e00467.
[59] Owens DK, Wendt RC. Estimation of the surface free energy of polymers. J Appl Polym Sci 1969;13:1741–7. https://doi.org/10.1002/app.1969.070130815.
[60] Berg S, Kutra D, Kroeger T, Straehle CN, Kausler BX, Haubold C, et al. ilastik: interactive machine learning for (bio)image analysis. Nat Methods 2019;16:1226–32. https://doi.org/10.1038/s41592-019-0582-9.
[61] ASTM D3039/D3039M. Standard test method for tensile properties of polymer matrix composite materials. West Conshohocken: ASTM International; 2017. https://doi.org/10.1520/D3039_D3039M-17.
[62] ASTM D790-03. Standard test methods for flexural properties of unreinforced and reinforced plastics and electrical insulating material. ASTM International; 2017.
[63] NF EN ISO 179-1 June 2010, Plastics - determination of Charpy impact properties - Part 1: non-instrumented impact test n.d.
[64] Shankar Tumuluru J, Sokhansanj S, Hess JR, Wright CT, Boardman RD. A review on biomass torrefaction process and product properties for energy applications. Ind Biotechnol 2011;7:384–401. https://doi.org/10.1089/ind.2011.7.384.
[65] Krevelen DW van, Nijenhuis K te. Properties of polymers: their correlation with chemical structure: their numerical estimation and prediction from additive group contributions. 4th, completely revised edition ed. Amsterdam: Elsevier; 2009.
[66] Zhang S, Sun X, Ren Z, Li H, Yan S. The development of a bilayer structure of poly(propylene carbonate)/poly(3-hydroxybutyrate) blends from the demixed melt. Phys Chem Chem Phys 2015;17:32225–31. https://doi.org/10.1039/C5CP06076A.
[67] Charlet K, Baley C, Morvan C, Jernot JP, Gomina M, Bréard J. Characteristics of Hermès flax fibres as a function of their location in the stem and properties of the derived unidirectional composites. Compos Appl Sci Manuf 2007;38:1912–21. https://doi.org/10.1016/j.compositesa.2007.03.006.